Appl Phys A (2012) 109:299–306
DOI 10.1007/s00339-012-7054-8

**Applied Physics A**
**Materials Science & Processing**

# Effects of silicon nanowires length on solar cells photovoltaic properties

**M. Farangi · M. Zahedifar · M.R. Mozdianfard · M.H. Pakzamir**

Received: 28 March 2012 / Accepted: 4 July 2012 / Published online: 18 July 2012


**Abstract** Silicon nanowires (SiNWs) were produced by an electroless method on FZ-Si (100) wafer, in $HF/AgNO_3$ solution. The influence of etching time and temperature on SiNWs morphology were studied using FESEM images. Optical properties were also investigated by optical absorption spectroscopy and low-temperature photoluminescence at 4.2 K. Considering their role as active regions, photovoltaic properties of SiNWs solar cells were studied for their different lengths. Photovoltaic measurements were taken in 1 sun condition under AM 1.5 illumination supplied by a solar simulator. Measurements indicated a reduction in efficiency as SiNWs length increased, which might be attributed to increased dangling states on nanowires surfaces.

## 1 Introduction

Considering the ever-increasing energy consumption trends worldwide, scientists are continuously looking for clean and renewable sources of energy such as capturing solar energy by solar cells. Hence, fabrication of solar cells made from one-dimensional nanostructures, has attracted a great deal of interest amongst researchers as cost-effective and highly efficient devices. Their physical properties, however, depend on their nanoscale dimensions, and as such, they provide good application potential in third-generation solar cells for which researchers investigate their electrical and optical properties as their dimensions changes [1–11]. SiNWs arrays on silicon substrate indicate high optical absorption because of strong light trapping by multiple scattering of the incident light among SiNWs and the optical antenna effect [12–15]. This causes very low reflectance and eliminates antireflective coating step required in the manufacturing process, thereby reducing the production cost of solar cell. Amongst different methods reported previously for fabricating SiNWs, in this study electroless method is employed as a simple and low-cost technique for large scale production of SiNWs on silicon substrate, where the desired growth direction and doping level of SiNWs can be achieved by proper selection of the silicon substrate. Then the effect of reaction time and temperature on morphology and length of SiNWs are studied and finally the photovoltaic properties of the fabricated SiNWs-based solar cells are examined.

## 2 Experimental

In this work, P-type monocrystalline FZ-Si (100) with resistivity around 1.5–4 Ω cm from Siltronic was used as raw wafer. The silicon samples were cut into $1 \times 1$ cm$^2$ and cleaned by immersing them into acetone, ethanol and HF (5 M) as well as de-ionized (DI) water for 10 min each, before etching in a sealed Teflon vessel using a HF (5 M) and $AgNO_3$ (0.02 M) solution [15–17]. To investigate the effect of reaction time, experiments were conducted between 10 min to 70 min. Having selected the reaction time of 60 min, the effect of temperature was investigated by tests at 40, 45, 50, 55, 60 and 65 °C. SiNWs growth was studied using a FESEM (Hitachi S-4160) images.

M. Farangi · M. Zahedifar · M.R. Mozdianfard · M.H. Pakzamir
Institute of Nanoscience and Nanotechnology, University of Kashan, Kashan, Iran

M. Zahedifar (✉)
Faculty of Physics, University of Kashan, Kashan, Iran
e-mail: zhdfr@kashanu.ac.ir

M.R. Mozdianfard
Chem. Eng. Dep., University of Kashan, Kashan, Iran

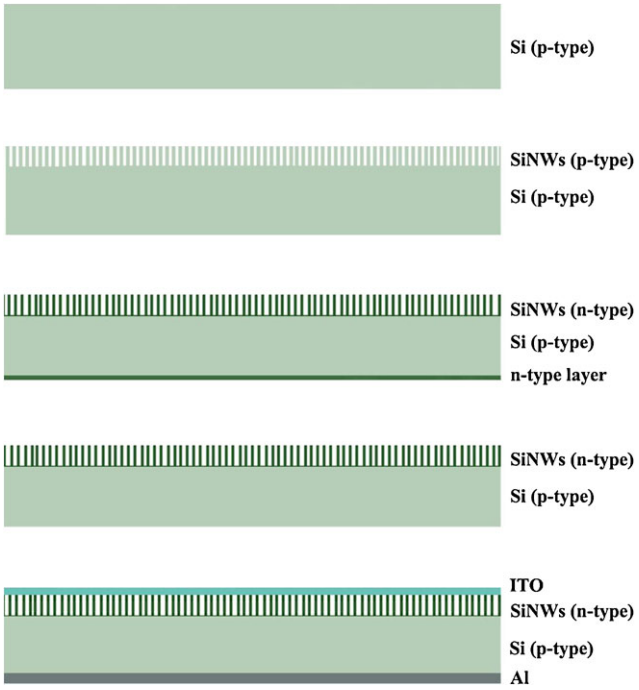


**Fig. 1** Schematic view of the fabrication process of SiNWs solar cell

Optical absorption spectroscopy was carried out within the wavelength range 200–800 nm using a Cary 500 spectrophotometer. The photoluminescence (PL) measurements were carried out using liquid helium-bath cryostats with glass windows. Band-to-band optical transition were provided using a 405 nm line of a 180 mV solid state laser as the excitation source. The monochromator was a 60 cm single grating with 600 grooves/mm. The PL signals were detected by an InGaAs p-i-n detector (Hamamatsu, Japan) and signal amplification was based on lock-in technique.

Figure 1 illustrates the schematic view of fabrication process of SiNWs solar cells in this work. Solar cells were fabricated using the common tube diffusion technique performed by $POCl_3$ at 900 °C for 120 min in nitrogen atmosphere. Therefore, P from $POCl_3$ diffuses into the P-type wafer (Fig. 1b) upon entry to the furnace, thereby changing it to n-type wafer where for its high density these are referred to as emitter layers. However, since the rear emitter layer was already an n-type, the post-diffusion wafer becomes an n-p-n type (Fig. 1c). The n-type rear emitter layer was then removed from the back surface of diffused wafer by HF, $H_2SO_4$, $HNO_3$, and $H_2O$ solution, making the final wafer an n-p type wafer (Fig. 1d). 100 nm indium tin-oxide (ITO) and 100 nm aluminum were deposited on silicon surfaces by sputtering and thermal evaporation methods as front and rear electrodes, respectively (Fig. 1e). Finally, the photovoltaic measurements were accomplished by solar simulator (Luzchem) and IVIUMSTAT (IVIUM) under AM1.5 condition.

## 3 Results and discussions

Temperature is an important factor in electroless process, controlling the nucleation rate of silver nanoclusters on silicon wafer, and hence its role had to be studied carefully in this research. Nucleation of silver nanoclusters is an important step in the electroless technique and determines the extent of surface etching and density of nanowires on substrate. Figure 2, illustrate the FESEM images of SiNWs formation at different temperatures and 60 min reaction time. As can be seen, many belt-like connections have been formed within the Si nanostructures at 40 °C, (see Fig. 2a and the inset). At this temperature, silver nucleation on silicon wafer does not seem to be substantial [15–17]. Hence, pores provided by Ag nanoparticles in silicon wafer do not meet each other, causing in effect these belt-like attached nanowires. A closer examination of Fig. 2 indicates that increasing temperature up to 55 °C, has improved nucleation; single SiNWs are formed on substrate around 50 °C and 55 °C, but with further rise in temperature, nucleation seems to have decreased and belt-like connections amongst SiNWs are observed again at 65 °C. Therefore, 55 °C was considered as the optimum temperature for SiNWs fabrication at 60 min reaction time in subsequent experiments. To ensure the correctness of the 60 min reaction time, a set of experiments were carried out at 55 °C production temperature and 10 to 70 min reaction times and Figs. 3–4 illustrate top and cross-section view FESEM images of SiNWs nanostructures, respectively. Nucleation of silver nanoclusters depends strongly on $AgNO_3$ concentration and temperature. As can be seen from Fig. 3, the concentration of SiNWs on silicon surface does not seem to have changed significantly at different reaction times. For clarity, different scales have been employed in Fig. 4. SiNWs length clearly depends on reaction (etching) time and this is better illustrated in Fig. 5, where the SiNWs length seems to be almost a linear function of reaction time. It seems that during redox reaction, silver atoms diffuse into Ag nanoparticles, and these nanoparticles sink into the Si wafer, sinking more and more into the silicon substrate [15–17]. Ag behavior as catalyst leads to formation of a SiNWs layer with specific length on the silicon surface, according to the following reactions:

$$Ag^+ + e^- \rightarrow Ag \quad (1)$$

$$Si + 6F^- \rightarrow SiF_6^{2-} + 4e^- \quad (2)$$

At this stage, SiNWs reflection of light for different incident wavelengths had to be investigated to verify the potential absorption for solar cell application. Figure 6 shows reflection spectra for different reaction temperatures in the

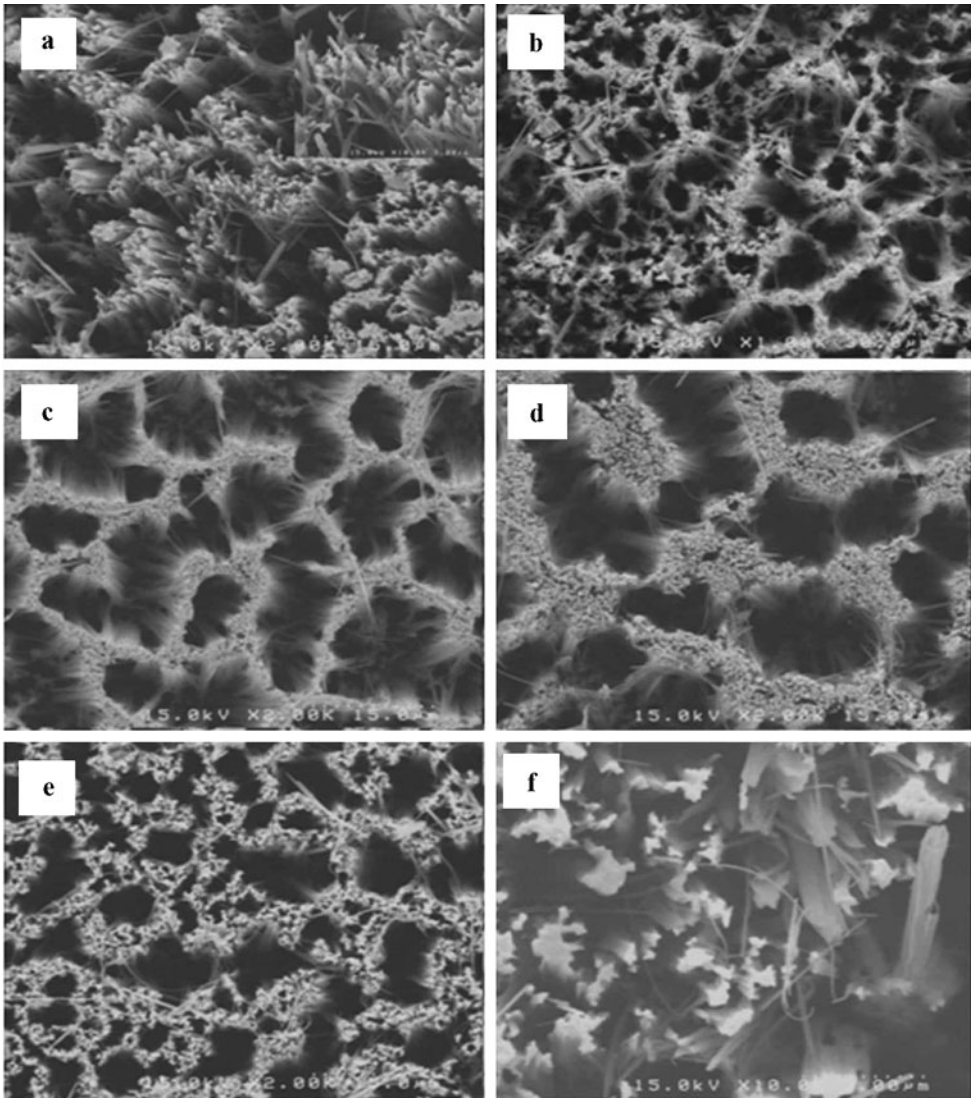


**Fig. 2** FESEM images of SiNWs produced by electroless method at 60 min reaction time and different temperatures of (**a**) 40 °C, (**b**) 45 °C, (**c**) 50 °C, (**d**) 55 °C, (**e**) 60 °C, (**f**) 65 °C

range of 200–800 nm. According to this figure, SiNWs have lower reflection than belt-like attached nanowires. Figure 7 demonstrates the reflection of SiNWs prepared at different reaction times (and hence different lengths) exposed to the spectrophotometer light (wavelength ranging from 200–800 nm). Shorter reaction times (i.e. less than 10 min), yielded unetched parts on silicon wafers (Figs. 3a and 3b) and shorter nanowires (Figs. 4a and 4b), leading to lower antireflection properties. Compared to a polished silicon wafer which has reflection ranging approximately from 90 to 40 % in these light wavelengths, clearly a significant reduction in reflection (from 0.25 to 2 %) is experienced for all SiNWs samples tested, confirming the antireflection properties of the SiNWs for this application. However, it is worth noting that increasing etching time and consequently SiNWs length reduces the reflection, be it to a small degree compared to the polished silicon wafer. This behavior could be explained by increased multiple scattering of photons within the longer SiNWs. It should be noted that the reflectivity of the polished wafer in our results, is slightly higher than what is calculated in the literature [18]. This could well be contributed to our experimental errors. As far as PL measurement is concerned, a test was carried out on a sample of 18 μm SiNWs on silicon wafer. The PL spectrum of *SiNWs* on Si substrate is demonstrated in Fig. 8. In the near-band-gap region (1.0–1.2 eV) clearly several somewhat narrow lines are seen, with one intense line at 1.09 eV. These lines correspond to the intrinsic excitonic emission from Si substrate ($FE^{TA}$, $FE^{TO}$ and so on) [19]. The broad emission band around energy ~1.17 eV is most likely due to electron-hole recombination on *SiNWs*.

To investigate the photovoltaic properties of SiNWs, seven samples, each with surface area 1 $cm^2$ and different lengths of 1.5, 8, 18, 28, 37, 44 and 51 μm were produced. As mentioned above, by decreasing the reaction time, shorter nanowires are obtained. However, these nanowires

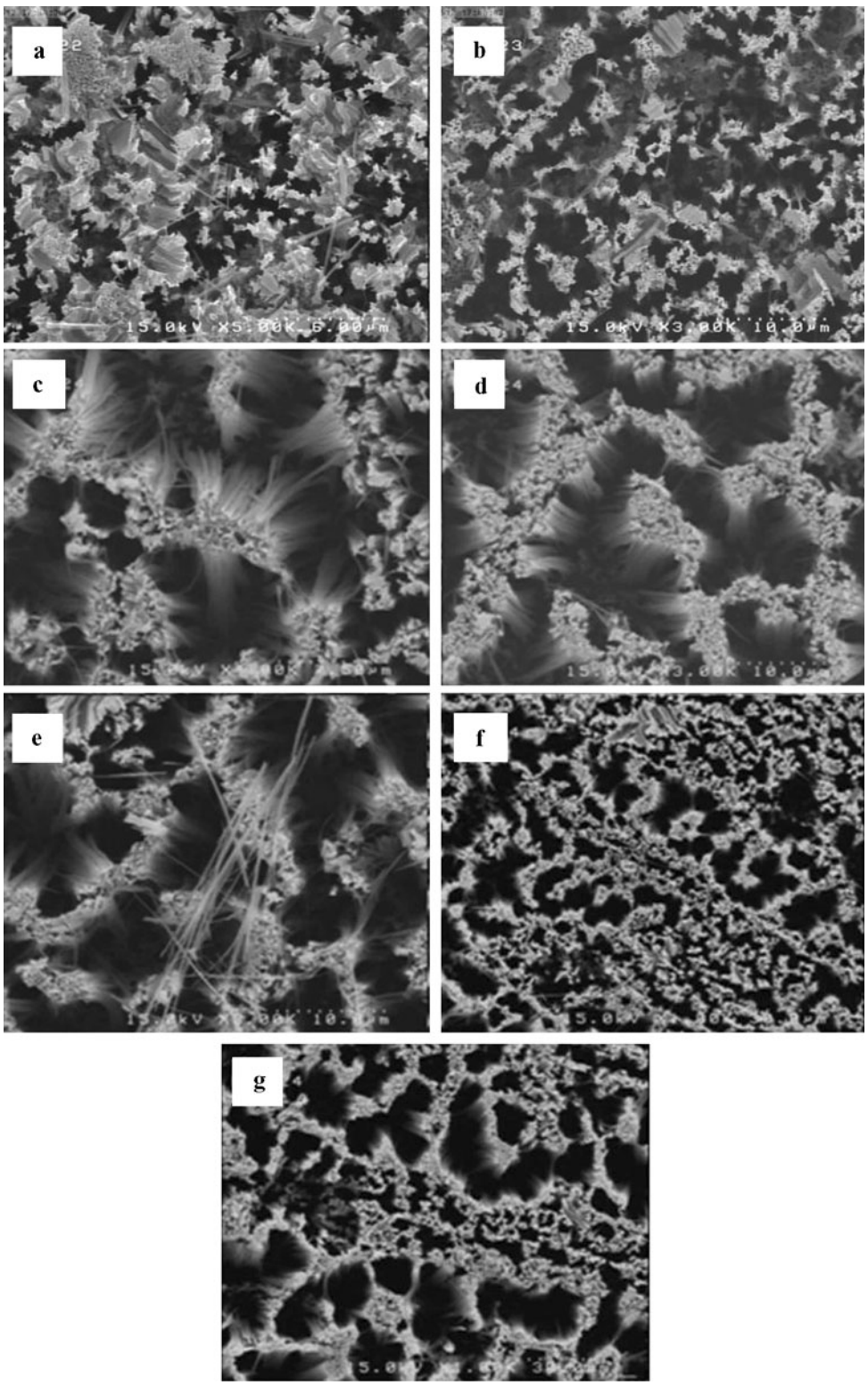


**Fig. 3** FESEM images (top view) of SiNWs produced by electroless method for different reaction times at 55 °C and operating temperatures of (**a**) 10 min, (**b**) 20 min, (**c**) 30 min, (**d**) 40 min, (**e**) 50 min, (**f**) 60 min, and (**g**) 70 min

are heterogeneously distributed on the surface having different forms of nanostructures and lower antireflection properties compared with longer nanowires. It is worth noting that shorter SiNWs than 1.5 μm resulted in unacceptable heterogeneity and uniformity in shape and as such 1.5 μm was selected as the minimum length in this work. Also, considering the characteristics of electroless method, and based on our experience here, the diameter and shape of the produced SiNWs cannot be controlled adequately using this fabrication method. Perhaps other methods such as lithogra-

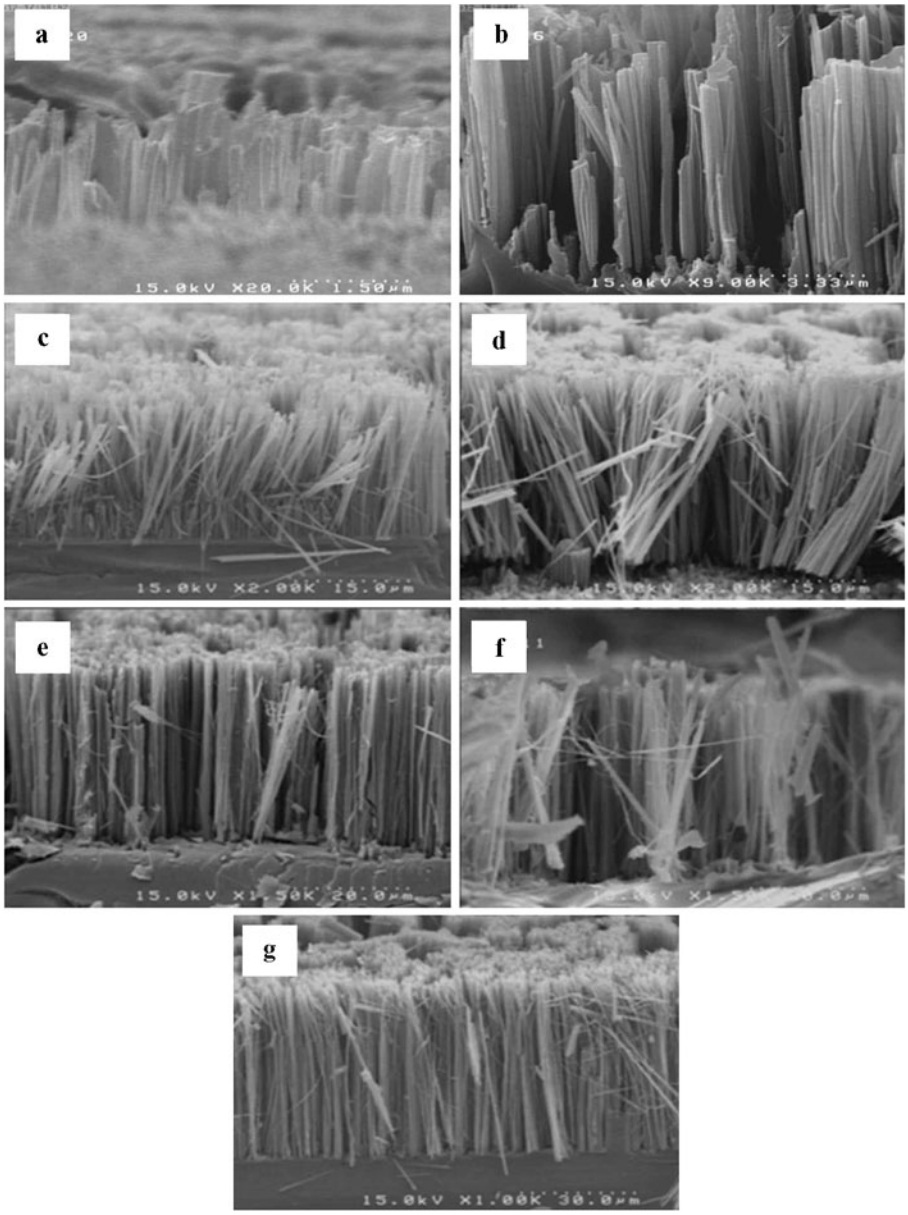


**Fig. 4** FESEM images (cross-section view) of SiNWs produced by electroless method for different reaction times at 55 °C and the same operating temperature as Fig. 2. Note that the scales are different in each image

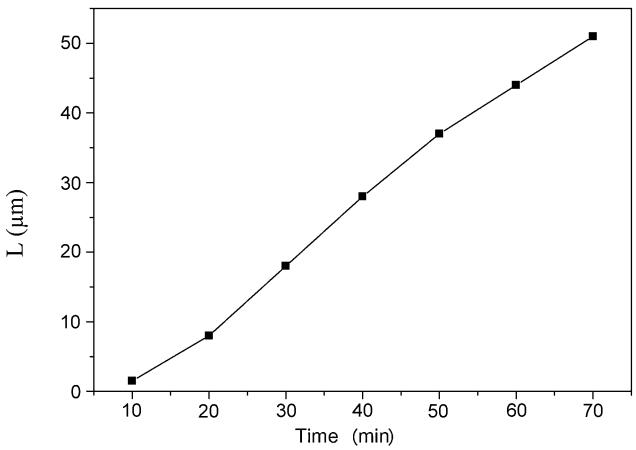


**Fig. 5** Variation of SiNWs lengths versus etching time from 10 min to 70 min and reaction time of 55 °C

phy may be employed for this. $I$–$V$ diagrams of these solar cells (see Fig. 9) indicate a linear behavior, which is different from the conventional ones and corresponds to low fill factors and reduced efficiency. The efficiency ($\eta_{\mathrm{AM1.5}}$ %) and fill factor ($FF$ %) of the solar cells may, respectively, be calculated as follows:

$$\eta_{\mathrm{AM1.5}}\,\% = \frac{P_{\mathrm{m}}}{P_{\mathrm{L}}} \times 100 = \frac{I_{\mathrm{m}} \cdot V_{\mathrm{m}}}{P_{\mathrm{L}}} \times 100 = \frac{I_{\mathrm{SC}} \cdot V_{\mathrm{OC}} \cdot FF}{P_{\mathrm{L}}} \times 100 \tag{3}$$

$$FF\,\% = \frac{I_{\mathrm{m}} \cdot V_{\mathrm{m}}}{I_{\mathrm{SC}} \cdot V_{\mathrm{OC}}} \times 100 \tag{4}$$

where $P_{\mathrm{m}} = I_{\mathrm{m}} \cdot V_{\mathrm{m}}$ is the maximum power output of solar cells ($I_{\mathrm{m}}$ and $V_{\mathrm{m}}$ correspond to current and voltage at the

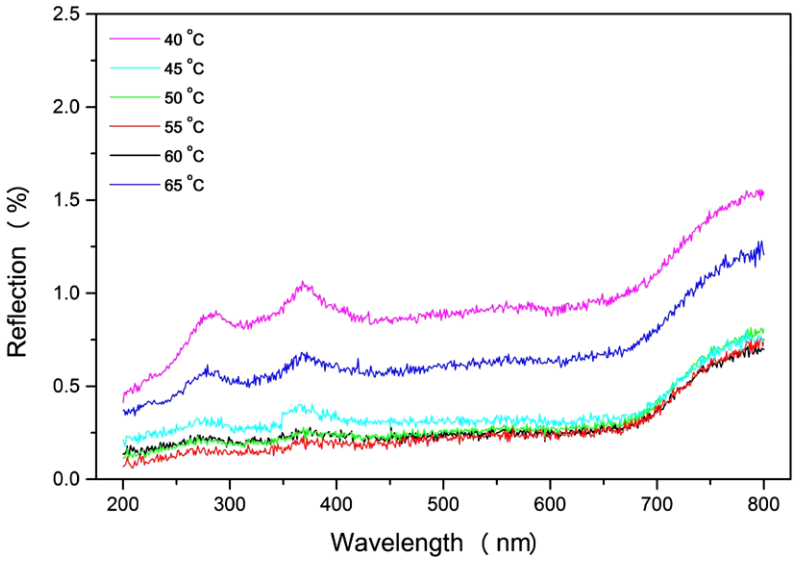


**Fig. 6** Reflection spectra of SiNWs produced with different reaction temperatures

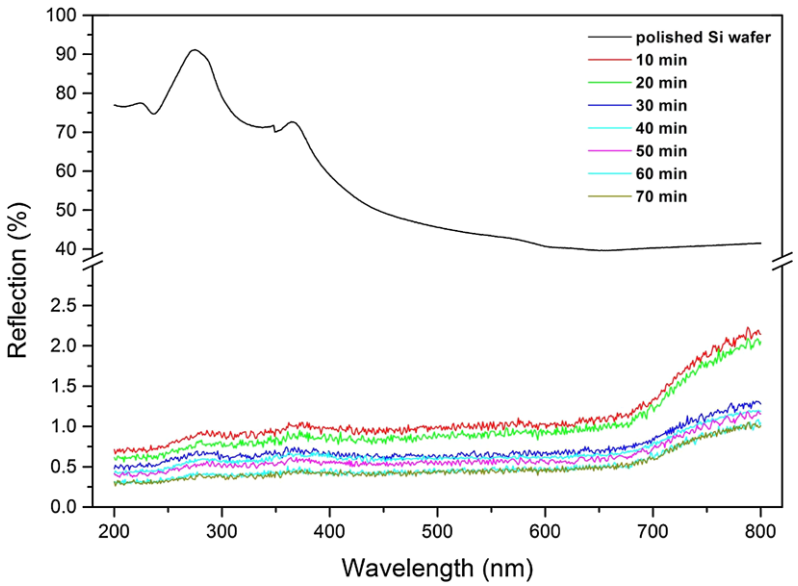


**Fig. 7** Reflection spectra of SiNWs produced with different reaction times

point of maximum power), $P_L$ is the power of incident, *FF* is the fill factor of solar cell in %, $I_{SC}$ and $V_{OC}$ are short circuit current (in mA) and open circuit voltage (in V) of the solar cell, respectively. It should be noted, however, that due to lack of access to vacuum facilities the experiments were carried out here in atmospheric environment, which is susceptible to oxidation at junctions. It is therefore suggested that low *FF* and efficiency experienced here could be attributed to poorly qualified junction formed between front electrode and SiNWs leading to a considerable amount of series resistance in the device configuration. Different characteristics of the solar cells prepared are summarized in Table 1, where a decrease in the solar cell efficiency is observed as SiNWs length is increased. This behavior is thought to be associated with the increased dangling states occurred on longer SiNWs, acting as recombination centers for light generated excitons.

Hence, the present study reveals two conflicting influences of the using SiNWs as far as photovoltaic properties of the fabricated solar cells are concerned. Firstly, they reduced substantially the reflection of light, thereby eliminating the need to employ antireflective coatings. Secondly, application of SiNWs increases the surface to volume ratio of the silicon structure, which in turn highlights the influence of surface defects acting as recombination sites. Meanwhile, carriers recombination depends strongly on the quasi levels on the SiNWs surface (which sets an upper limit for open circuit voltage), $V_{OC}$ therefore, declines by escalation of re-

combination rate (Fig. 9). The resulting decreased reflection, and increased recombination rate (reduced $J_{SC}$ and $V_{OC}$) call for procedures such as passivation to reduce the recombination rate and this too should be investigated in further studies to improve the photovoltaic response.

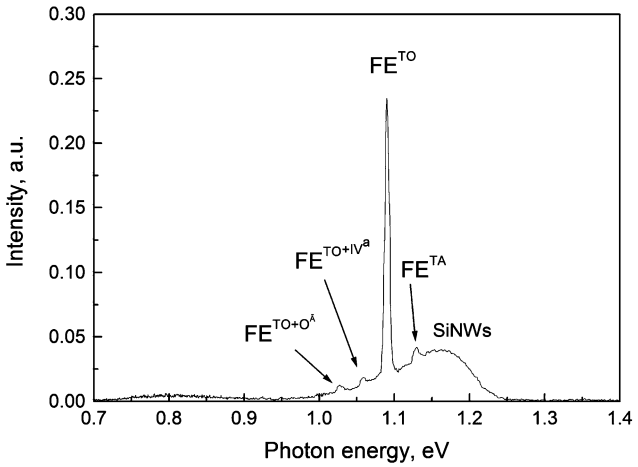


**Fig. 8** Low-temperature PL spectrum of SiNWs on silicon wafer at 4.2 K

## 4 Conclusions

In this work, having considered SiNWs growth on FZ-silicon wafer by electroless technique, an optimum temperature of 55 °C for etching process was determined. SiNWs length was found to depend strongly on the reaction time, while their concentration does not seem to change significantly with reaction time. Optical absorption spectroscopy confirms the antireflective potentials of SiNWs, which is enhanced gradually by increase in nanowires length. Low-temperature PL at 4.2 K indicated the band energy of almost 1.17 eV related to SiNWs. A decreasing trend in efficiency of solar cells was experienced with longer SiNWs. This behavior is thought to be associated with increased dangling states and defects on SiNWs surfaces highlighted by the increased length of SiNWs. In applying SiNWs, the decreased reflection, and increased recombination rate (reduced $J_{SC}$ and $V_{OC}$) not only call for an optimum length of SiNWs, but also passivation technique, to improve the photovoltaic response.

**Acknowledgements** The authors gratefully acknowledge the financial support of research council, at the University of Kashan, and Prof. V.F. Gremenok of 'Belarusian Academy of Science' for his technical assistance with photoluminescence measurements.

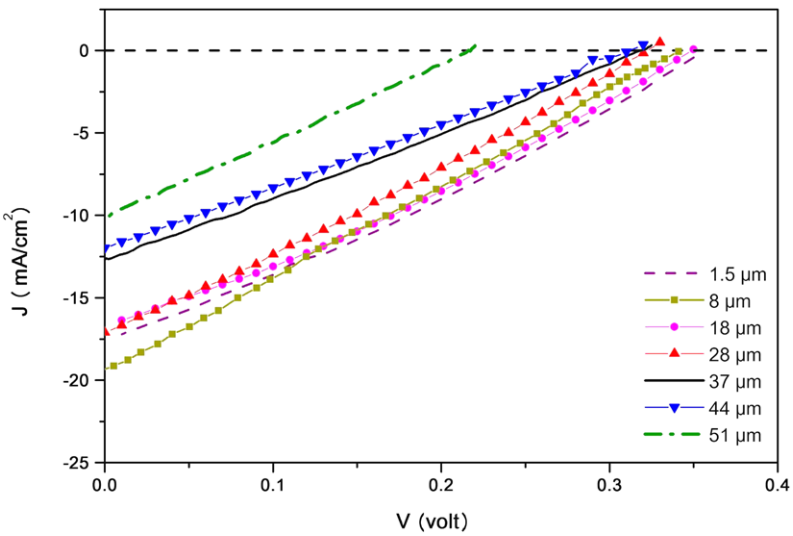


**Fig. 9** $I$–$V$ diagrams of SiNWs solar cells, 1 $cm^2$ surface area and different nanowires lengths

**Table 1** Photovoltaic characteristics of solar cells for different nanowires lengths

| NWs length (μm) | $V_{OC}$ (V) | $J_{SC}$ (mA/cm$^2$) | *FF* % | $\eta$ % |
|---|---|---|---|---|
| 1.5 | 0.35 | 17.2 | 30 | 1.81 |
| 8 | 0.34 | 18.77 | 26.25 | 1.68 |
| 18 | 0.34 | 16.37 | 29.27 | 1.63 |
| 28 | 20.32 | 17.11 | 27.26 | 1.49 |
| 37 | 0.32 | 12.70 | 26.55 | 1.07 |
| 44 | 0.31 | 11.99 | 26.04 | 0.97 |
| 51 | 0.22 | 10.15 | 25.94 | 0.57 |

## References


1. Y. Cui, Q. Wei, H. Park, C.M. Lieber, Science **293**, 1289 (2001)
2. M. Marsen, K. Sattler, Phys. Rev. B **60**, 11593 (1999)
3. Q. Li, S.M. Koo, M.D. Edelstein, J.S. Suehle, C.A. Richter, Nanotechnology **18**, 315202 (2007)
4. F. Patolsky, G. Zheng, C.M. Lieber, Nat. Protoc. **1**, 1711 (2006)
5. M. Hernandez-Velez, Thin Solid Films **495**, 51 (2006)
6. P. Chaudhari, H. Shim, B.A. Wacaser, M.C. Reuter, C. Murray, K.B. Reuter, J. Jordan-Sweet, F.M. Ross, S. Guha, Thin Solid Films **518**, 5368 (2010)
7. Z. Li, B. Rajendran, T.I. Kamins, X. Li, Y. Chen, R.S. Williams, Appl. Phys. A, Mater. Sci. Process. **80**, 257 (2005)
8. L.A. Jones, G.M. Taylor, F.X. Wei, D.F. Thomas, Prog. Surf. Sci. **50**, 283 (1995)
9. N. Fukata, T. Oshima, N. Okada, T. Kizuka, T. Tsurui, S. Ito, K. Murakami, Physica B **864**, 376–377 (2006)
10. Y.H. Tang, Y.F. Zhang, N. Wang, C.S. Lee, X.D. Han, I. Bello, S.T. Lee, J. Appl. Phys. **85**, 7981 (1999)
11. K.Q. Peng, Z.P. Huang, J. Zhu, Adv. Mater. **16**, 73 (2004)
12. Th. Stelzner, M. Pietsch, G. Andrä, F. Falk, E. Ose, S. Christiansen, Nanotechnology **19**, 295203 (2008)
13. L. Hu, G. Chen, Nano Lett. **7**(11), 3249 (2007)
14. K. Peng, Y. Xu, Y. Wu, Y. Yan, S.T. Lee, J. Zhu, Small **1**, 1062 (2005)
15. J.Y. Jung, Z. Guo, S.W. Jee, H.D. Um, K.T. Park, J.H. Lee, Opt. Express **18**, 286 (2010)
16. G. Kalita, S. Adhikari, H.R. Aryal, R. Afre, T. Soga, M. Sharon, W. Koichi, M. Umeno, J. Phys. D, Appl. Phys. **42**, 1 (2009)
17. S.D. Hutagalung, A.S.Y. Tan, R.Y. Tan, Y. Wahab, Proc. SPIE **7743**, 1 (2010)
18. L. Hu, G. Chen, Nano Lett. **7**(11), 3249–3252 (2007)
19. A.V. Mudryi, A.I. Patuk, I.A. Shakin, A.G. Ulyashin, R. Job, W.R. Fahrner, A. Fedotov, A. Mazanik, N. Drozdov, Sol. Energy Mater. Sol. Cells **72**, 503 (2002)